Nanotechnology **20** (2009) 505301 (5pp) doi:10.1088/0957-4484/20/50/505301

Controlled fabrication of individual silicon quantum rods yielding high intensity, polarized light emission

Benjamin Bruhn[1], **Jan Valenta**[2] **and Jan Linnros**[1]

[1] Materials Physics, School of ICT, Royal Institute of Technology, Electrum 229, S-16440 Kista-Stockholm, Sweden
[2] Department of Chemical Physics and Optics, Faculty of Mathematics and Physics, Charles University, Ke Karlovu 3, 12116 Prague 2, Czech Republic

E-mail: bbruhn@kth.se

Received 22 September 2009, in final form 27 October 2009
Published 19 November 2009
Online at stacks.iop.org/Nano/20/505301

Abstract
Elongated silicon quantum dots (also referred to as rods) were fabricated using a lithographic process which reliably yields sufficient numbers of emitters. These quantum rods are perfectly aligned and the vast majority are spatially separated well enough to enable single-dot spectroscopy. Not only do they exhibit extraordinarily high linear polarization with respect to both absorption and emission, but the silicon rods also appear to luminesce much more brightly than their spherical counterparts. Significantly increased quantum efficiency and almost unity degree of linear polarization render these quantum rods perfect candidates for numerous applications.

1. Introduction

Light emission properties of nanostructured silicon have been known since the 1980s [1, 2] while the general interest of the scientific community was increased by the discovery of strong luminescence from porous silicon [3, 4]. The effect was earlier associated with quantum confinement of excited carriers in small silicon nanocrystallites, but direct proof was not obtained until single nanocrystal spectroscopy studies were undertaken [5–7]. Indeed, a line narrowing of the emission peak at low temperatures to less than k_BT ($\sim$2 meV at 35 K) [8] as well as individual peak emission energies due to size dispersion yield strong evidence for the quantum confinement model. In addition, the observation of on/off blinking [9], as observed, for example, for CdSe nanocrystals [10], yields further support for the concept of a silicon quantum dot.

While the quantum efficiency of the luminescence is quite high [11], time-resolved measurements yield lifetimes in the microsecond regime due to the indirect nature of the bandgap. This generally limits the brightness of the emission, as strong excitation usually results in fast Auger recombination whenever several excitons are present in a single nanocrystal.

When the spherical symmetry of a quantum dot is broken, many interesting effects appear, a few of which are polarized light emission, faster radiative recombination and even a suppression of Auger recombination [12]. For such 'quantum rods' Shabaev and Efros [13] introduced a 1D exciton model explaining available data for CdSe nanorods such as a very high polarization degree. For porous silicon polarization effects have been observed [14], in part explained by the dielectric confinement as a result of the wire-like network of the remaining silicon skeleton.

In this paper we report on the reliable fabrication of silicon quantum rods utilizing electron beam lithography (EBL), reactive ion etching (RIE) and a subsequent oxidation. The first two steps yield standing wall-like structures, whereas the oxidation finalizes our nanostructures by oxidizing through the supporting walls and shrinking the remaining silicon core at the top of the structures. Photoluminescence (PL) measurements and electron microscope images are used to argue in favor of the single-dot nature and elongated shape, i.e. quantum rods. We also attempt to explain the measured high intensity emission and extraordinarily high polarization.

2. Experimental details

The fabrication principle is similar to the ones used in earlier experiments [7, 8], except for the definition of lines instead

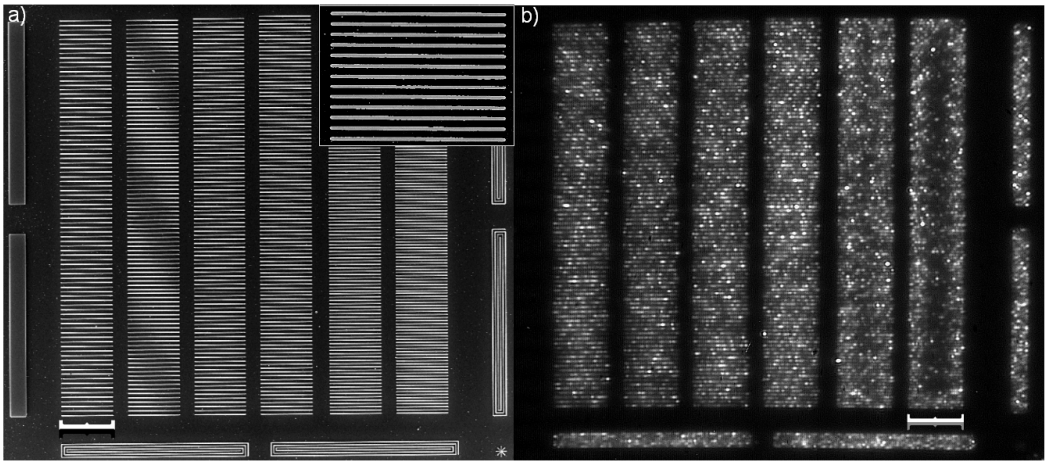

Figure 1. (a) SEM image of six columns of closely spaced silicon walls from top view. The inset shows a close-up. (b) PL image of the same structures after long oxidation. Due to closer spacing in the right-hand side columns oxidation rates were slightly lower, yielding less luminescence centers. (a), (b) Scale bars indicate 10 μm.

of dots with EBL. Silicon n-type (100) wafer pieces of 10 × 10 mm^2 with a resistivity of 20 Ω cm were oxidized at 1100 °C for 12 min, resulting in a top oxide layer of about 25 nm thickness. Positive resist ZEP520:Anisol (1:2) was spun onto the oxide layer at 1500 rpm. Then the resist was baked at 180 °C for 10 min. Line patterns were defined using EBL, which enables precise positioning. Then metal (NiCr) deposition, lift-off (in an ultrasonic acetone bath) and a wet etching step in diluted hydrofluoric acid (DHF) transferred the pattern into the silicon dioxide layer. The metal was removed and the remaining oxide used as a hard mask for plasma etching. After RIE the resulting silicon walls, being approximately 75 nm wide and 200 nm high, were oxidized at 900 °C. Oxidation for less than 8 h led to formation of undulating nanowires in the wall top, delimited from the substrate by complete oxidation through the walls, since built-up stress at convex curvatures reduces the local oxidation rate [15, 16]. Extended oxidation then yielded spatially well-separated luminescent nanocrystals through amplification of the aforementioned wire inhomogeneities.

The exact wall thickness and height, as well as the exact extended oxidation time, do not have a major influence on successful quantum rod fabrication, which is a great advantage compared to other methods such as oxidation of pillars [7, 8].

After fabrication, photoluminescence was excited in the nanocrystals by a slightly focused cw HeCd laser at 325 nm. The PL imaging set-up involved a microscope using a 100× objective with high numerical aperture (NA = 0.7), an imaging spectrometer and a liquid-nitrogen-cooled charge-coupled device (CCD) camera. In a second set-up, excitation with a 405 nm laser diode was used in an epifluorescence configuration (excitation and detection through the same lens). A double Fresnel rhomb and linear polarizer were used to rotate and clean the polarization of the laser beam. Another linear polarizer (analyzer) was placed after the objective lens to allow for polarization-sensitive detection. All results were cross-checked on both measurement systems with a variety of different samples.

3. Results and discussion

An example of a typical silicon wall pattern is shown in figure 1(a). Figure 1(b) shows a corresponding PL image of the same sample after 9 h of oxidation at 900 °C. Many spatially separated emission centers can clearly be seen in this picture. These show characteristic properties of single silicon quantum dots, as will be demonstrated below.

Before addressing the optical properties of these emitting dots we will examine their structure trying to identify the origin of the light emission. As detailed in section 2, the oxidation of the silicon walls at a relatively low temperature resulted in almost complete oxidation of the walls except for the top, where an undulating core of silicon remained. This is explained by an effect called self-limiting oxidation [15, 16] and is demonstrated in figure 2(b) for a sample after short oxidation. A bright silicon nanowire of diameter ∼20 nm can be seen in the wall top, separated from the bulk silicon by a somewhat transparent oxide.

In order to determine if the luminescence originates from such a rather thick wire, we examined the star-like structure (present on the same sample) displayed in figure 2(a) in detail. A PL image taken from this structure is shown in the inset. Comparing with the SEM image, horizontal and vertical arms host many more luminescing objects than diagonal walls. A cross-section cut with a focused ion beam (FIB) reveals the inner structure of those and allows clarification of the question at hand, i.e. the structure of the light-emitting centers. As can be seen from figure 2(d), which is taken at a high tilt angle to reveal the cross section of the walls, the non-luminescing diagonal arms contain intact nanowires of relatively large diameter ($\gtrsim$10 nm), whereas the luminescing arms dissected in figure 2(c) most likely only contain separated nanocrystals that are too small to see with an SEM. Note that the central core in figure 2(d) connecting the top wire with the substrate is completely removed by further oxidation (see figures 2(b) and (c)) and is not believed to contribute to the PL yield. These results were confirmed on numerous different samples. Thus,

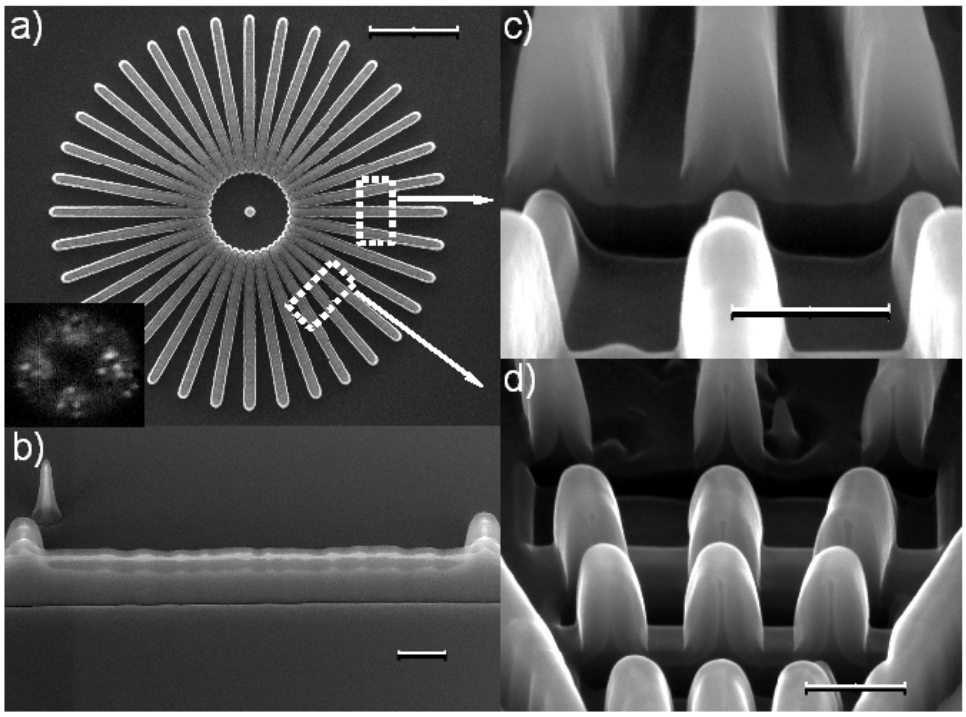

Figure 2. (a) SEM top view of silicon walls patterned like a star. Image was taken before oxidation. White dashed rectangles indicate parts used for cross sections in (c) and (d). Inset shows a PL image of such a star after long oxidation. In contrast to horizontal and vertical arms, the diagonal walls do not host quantum rods and therefore appear dark. This is very likely due to slower oxidation rate for this crystal direction. (b) SEM side view of an oxidized silicon wall. The center is oxidized through, while an undulating wire remains on top. No luminescence is obtained from it yet, since its radius of 15–25 nm is too large. (c) FIB/SEM cross section of horizontal (luminescing) arms. Luminescing nanorods are too small for the SEM to detect. (d) FIB/SEM cross section of diagonal (dark) arms. The wires are too large for visible luminescence and even still connected to the substrate at some points. (a) Scale bar indicates 2 μm. (b)–(d) Scale bars indicate 200 nm.

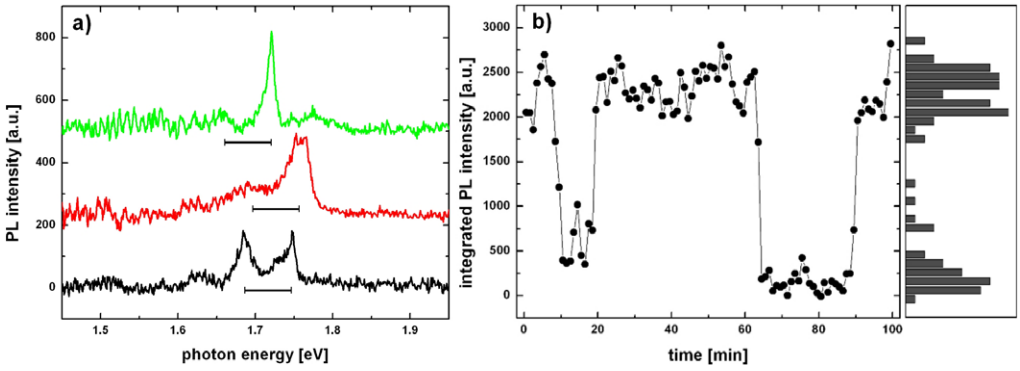

Figure 3. (a) Representative single-dot spectra at $T = 77$ K. Energy positions are slightly shifted and 60 meV TO-phonon replicas, indicated by scale bars, differ in strength. Peak widths approach thermal energy. (b) Blinking time trace of a single dot. The histogram to the right shows clear two-level (on/off) blinking on a minute scale.

we conclude that the luminescence originates from structures much smaller than those seen in SEM images, possibly in the few-nanometer range, as would be expected for silicon nanocrystals. Since these structures evolve from the nanowires (such as the one imaged in figure 2(b)) upon further oxidation, we propose, without definite proof at this stage, that their shape would most likely be elongated or rod-like, with their longer axis oriented along the length of the walls.

Turning to optical characteristics, we now demonstrate that the luminescing dots (cf figure 1(b)) exhibit true single quantum dot character. We therefore measured room temperature and low temperature spectra as well as emission intermittency for many of the emitting objects. It was found that most of them blink on a second to minute scale, with intensity levels limited to two states, on and off. Figure 3(b) shows a blinking time trace of a selected dot and the corresponding intensity histogram. In figure 3(a) three representative spectra at liquid nitrogen temperature are displayed. While room temperature measurements usually yield a peak width of 100–150 meV, these spectra yield linewidths of ∼10 meV, approaching the thermal energy $k_B T$ at 77 K. TO-phonon replicas are usually observed with different

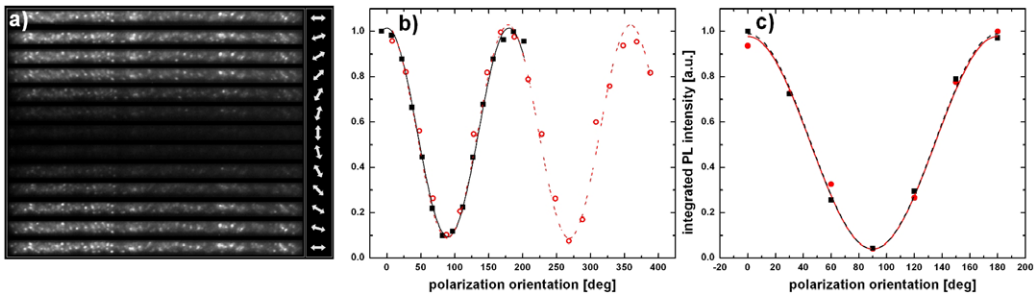

Figure 4. (a) PL images of a horizontal pattern consisting of six closely spaced oxidized silicon walls. White arrows indicate polarization filter orientation. Only light polarized parallel to the filter can be detected. (b) Emission (black squares) and absorption (red circles) polarization data for an ensemble. Sinusoidal fits yield DLP of 0.84 and 0.83, respectively. (c) Absorption and emission polarization for a single dot. Both DLP are 0.92, which is representative. Some dots exhibit values of up to 0.97. The difference in (b) and (c) can be explained by small angular variations of the nanorod orientations paired with difficulties in background subtraction.

(This figure is in colour only in the electronic version)

intensities with respect to the main line, but the reason for this characteristic feature is not understood yet. Kovalev *et al* [17] argued that the ratio of no-phonon to TO-phonon peaks depends on nanocrystal size and passivation. It is likely that the nanocrystal shape also plays a role here.

We now address polarization effects. A number of publications suggest that elongated nanocrystals (rods) exhibit a much higher degree of linear polarization (DLP) than spherical ones [12, 18, 19], which has been confirmed for other semiconductor nanorods [20, 21] and, to a certain extent, also for porous silicon [22]. To the authors' knowledge, only in one article [23] was an extraordinarily high DLP found for silicon nanorods, but the preparation method does not allow for single-dot spectroscopy.

Photoluminescence measurements on ensembles as well as on single dots were performed in order to determine their absorption and emission polarization. Figure 4(a) is a composite image of 13 PL images, taken at various polarization angles (indicated by arrows) of a wall structure hosting numerous single silicon quantum dots. As becomes clear from this experiment, all dots emit light that is exclusively polarized along the wall direction. The corresponding data is plotted in figure 4(b) for ensemble measurements, while the data in figure 4(c) reveal an even higher degree of polarization for a single dot. The degree of polarization as indicated in the caption is defined as $(I_{\max} - I_{\min})/(I_{\max} + I_{\min})$, where $I_{\max}$ and $I_{\min}$ are defined as the maximum and minimum intensities of the fitted sinusoidal curve. Indeed, the observed almost complete polarization of both absorption and emission gives further support to an elongated rod-like shape of the emitting nanocrystals.

If the elongated quantum dots are treated as infinitely long cylinders and if their up to 50 nm thick oxide shell is neglected so that the surrounding medium is air, macroscopic electromagnetic theory (dielectric confinement) accounts well for the observed high DLP values. However, it is questionable that this approach holds [19], especially with regard to other properties found in semiconductor nanorods, such as large non-monotonic Stokes shifts for increasing aspect ratio [12]. It has therefore been proposed that the extraordinarily high polarization is caused by formation of one-dimensional excitons (1DE) [13]. Not only do this theory and earlier approaches [12] explain high absorption and emission polarization ratios for nanorods, they also predict a number of other phenomena, of which the most interesting one might be increased emission yield due to higher quantum efficiency. Other publications support this idea, proposing explanations that are mostly connected to reduced Auger-assisted recombination rates (found for nanowires [24], but should be applicable to nanorods of sufficient elongation as well [18, 25]) and longer nonradiative lifetimes [26].

In our experiments we could observe that the acquisition time required for obtaining a sufficiently bright PL image was much shorter for a sample with oxidized silicon walls than for one with colloidal silicon quantum dots or dots from oxidized pillars [9]. In other words, our quantum rods do not only emit strongly polarized light, but they also yield light intensities higher by at least a factor of five than any spherical dots we can compare them with. This phenomenon can be understood in terms of a reduced efficiency of Auger-assisted recombination, as stated before, and is most likely aided by a combination of a shortened lifetime and an increased absorption cross section [18, 19, 13, 27].

4. Conclusion

We have developed a method for reliably fabricating spatially well-separated single silicon quantum rods utilizing electron beam lithography, plasma etching and oxidation. In different measurements we found strong support for an elongated shape of our nanocrystals, two of which are the extremely high linear absorption and emission polarization and a significantly higher emission intensity than observed for spherical silicon quantum dots. A decreased Auger-assisted recombination rate, shortened radiative lifetime and a larger absorption cross section may explain this increase in emission yield. All phenomena seem to be well accounted for by a 1D exciton model, which has proven to be valid for other types of semiconductor quantum rods.

Finally, both the increased brightness and the high polarization ratio, as well as their photostability, make silicon quantum rods with oxide passivation suitable for a range of

applications, among which are phosphors and fluorescence tagging of biomolecules and sensors.

Acknowledgments

Financial support from the Swedish Research Council (VR) through a Linné grant is gratefully acknowledged. Part of this work (JV) was supported through the research centre LC510 of MSMT and the project 202/07/0818 of the GACR.

References

[1] Di Maria D J, Kirtley J R, Pakulis E J, Dong D W, Kuan T S, Pesavento F L, Theis T N, Cutro J A and Brorson S D 1984 *J. Appl. Phys.* **56** 401
[2] Furukawa S and Miyasato T 1988 *J. Appl. Phys.* **27** L2207–09
[3] Canham L T 1990 *Appl. Phys. Lett.* **57** 1046
[4] Lehmann V and Gösele U 1991 *Appl. Phys. Lett.* **58** 856
[5] Mason M D, Credo G M, Weston K D and Buratto S K 1998 *Phys. Rev. Lett.* **80** 5405
[6] Mason M D, Sirbuly D J, Carson P J and Buratto S K 2001 *J. Phys. Chem.* **114** 8119
[7] Valenta J, Juhasz R and Linnros J 2002 *Appl. Phys. Lett.* **80** 1070
[8] Sychugov I, Juhasz R, Valenta J and Linnros J 2005 *Phys. Rev. Lett.* **94** 087405
[9] Sychugov I, Juhasz R and Linnros J 2005 *Phys. Rev.* B **71** 115331
[10] Efros Al L and Rosen M 1997 *Phys. Rev. Lett.* **78** 1110
[11] Linnros J, Lalic N, Galeckas A and Grivickas V 1999 *J. Appl. Phys.* **86** 6128
[12] Hu J, Li L-S, Yang W, Manna L, Wang L-W and Alivisatos A P 2001 *Science* **292** 2060
[13] Shabaev A and Efros Al L 2004 *Nano Lett.* **4** 1821
[14] Kovalev D, Ben Chorin M, Diener J, Koch F, Efros Al L, Rosen M, Gippius N A and Tikhodeev S G 1995 *Appl. Phys. Lett.* **67** 1585
[15] Marcus R B and Sheng T T 1982 *J. Electrochem. Soc.* **129** 1278
[16] Cui H, Wang C X and Yang G W 2008 *Nano Lett.* **8** 2731
[17] Kovalev D, Heckler H, Ben-Chorin M, Polisski G, Schwartzkopff M and Koch F 1998 *Phys. Rev. Lett.* **81** 2803
[18] Trani F, Cantele G, Ninno D and Iadonisi G 2005 *Phys. Rev.* B **72** 075423
[19] Trani F 2007 *Surf. Sci.* **601** 2702
[20] Wang J, Gudiksen M S, Duan X, Cui Y and Lieber C M 2001 *Science* **293** 1455
[21] Peng X, Manna L, Yang W, Wickham J, Scher E, Kadavanich A and Alivisatos A P 2000 *Nature* **404** 59
[22] Kovalev D, Averboukh B, Ben-Chorin M, Koch F, Efros Al L and Rosen M 1996 *Phys. Rev. Lett.* **77** 2089–92
[23] Ma D D D, Lee S T and Shinar J 2005 *Appl. Phys. Lett.* **87** 033107
[24] Guichard A R, Kekatpure R D, Brongersma M L and Kamins T I 2008 *Phys. Rev.* B **78** 235422
[25] Wang F and Buhro W E 2007 *J. Am. Chem. Soc.* **129** 14381
[26] Htoon H, Hollingsworth J A, Dickerson R and Klimov V I 2003 *Phys. Rev. Lett.* **91** 227401
[27] Kovalev D, Diener J, Heckler H, Polisski G, Künzner N and Koch F 2000 *Phys. Rev.* B **61** 4485–87